Notes on beam energy measurements at FNPL

P. Piot[1], N. Barov[2], T. Berenc[1], and Y.-E. Sun[3]
[1]*Fermilab, Batavia, IL 60510, USA*
[2]*Northern Illinois University,*
[3]*University of Chicago*

April 19, 2004

Abstract

The present note attempts to clarify the long standing topics of beam energy gain at FNPL. After a recalibration of the spectrometer magnet end of 2001, it was found that the beam energy was lower than what one would infer from the settings of the various radio-frequency components (the gun and the TESLA cavity). In this note we analyze these observations and propose a new rf-calibration (done with beam) for the rf-gun and the TESLA cavity.

1 Introduction

After re-installation of gun 4 on the FNPL beamline in Spring 2003, it was noticed that for given setting of the rf-gun and the TESLA cavity, the measured beam energy* downstream of the spectrometer was lower than the total one would expect from the forward power going into the gun cavity (the reflected power was checked to be approximately zero) and the transmitted power through the TESLA cavity.

A similar problem was indeed observed with gun 3 (installed from May 2002 to May 2003 in the FNPL beamline). However because of the lack of knowledge of the gun damage and resulting electric field un-balance, the reason for the lower energy was not investigated at that time.

Looking back at the history, when gun 4 was first installed in the FNPL beamline (e.g. in March 2002 [1]) we find that a total energy of $9.5 \times 1.614 \simeq 15.3$ MeV were routinely measured which would mean the beam total energy at the gun exit was about 3 MeV if one trust the rf-calibration of the TESLA cavity at that time (for the canonical setting point of the TESLA cavity of $V_t = 49.1$ mV on the transmitted power diode) the energy gain

*throughout this note we do the approximation, for the total energy, $E_{tot} = \sqrt{(pc)^2 + (m_e c^2)^2} \simeq pc$ wherein p is the beam momentum. At 3 MeV this results in an underestimate of 1% for E_{tot} while above 12 MeV this is a 0.1% error. This approximation only matters when comparing simulations with measurements.

was $12.0 \times 1.03 \simeq 12.3$ MeV. This energy of 3 MeV is inconsistent with expected energy (4.5 MeV) estimated from the forward power going into the gun (the forward power diode signal was $V_f \simeq 42$ mV)

In Figure 1 we present the expected total energy of the beam downstream of the beam versus peak accelerating field on the photo-cathode.

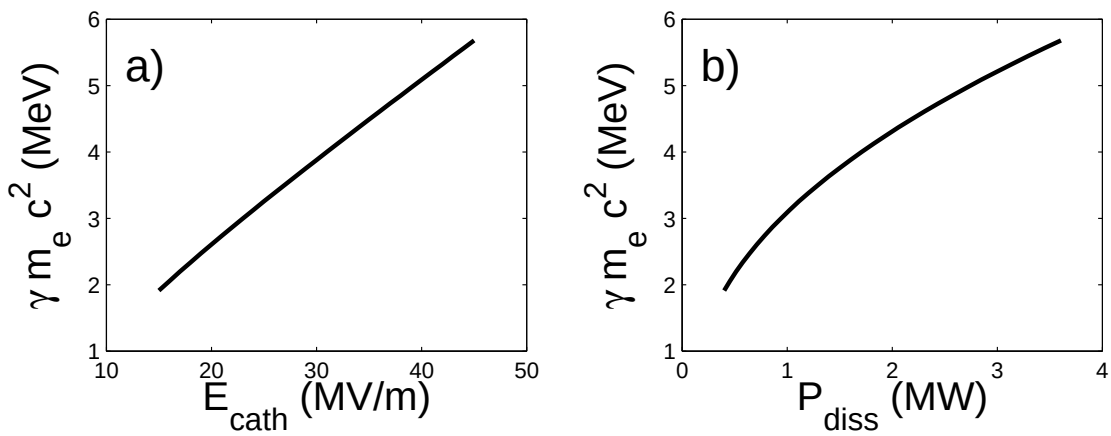

Figure 1: Total beam energy downstream of the gun versus peak electric field on the photo-cathode (a) and versus dissipated power in the cavity (b).

2 The TESLA cavity zero-gradient extrapolation technique

2.1 Principle of method

Because of the energy dependence of optical transition radiation (OTR) angular distribution, it is difficult to collect a large number of photons at energies of a few MeV. It is therefore not possible to diagnose the beam energy with the spectrometer when the TESLA cavity is turned off. Instead we inferred the beam energy at the gun exit from an indirect measurement: the beam energy is measured for different set-points of the TESLA cavity, and the thereby obtained dependence is extrapolated to zero accelerating field in the TESLA cavity. The total energy downstream of the TESLA cavity is given by:

$$E = E_g + eV_{rf} \cos\phi \doteq E_g + E_{TESLA}, \tag{1}$$

wherein E is computed from the spectrometer current and given the calibration provided in Reference [7], E_g is the total energy at the gun exit and V_{rf} is the accelerating voltage amplitude of the TESLA cavity. Hence the extrapolation of E versus E_{TESLA} line to $E_{TESLA} = 0$ provides a measurement of the rf-gun energy. Note that (1) the line intercept is insensitive to error in the rf-calibration of E_{TESLA} and (2) the line slope provides a quality check of the TESLA cavity rf-calibration with the spectrometer calibration it should be close to 1 (see annexe). It is important to estimate the order of magnitude of systematic errors that one

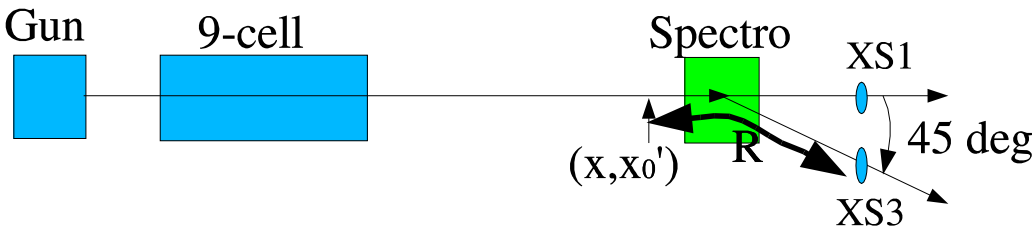

Figure 2: Setup to measure energy of fnpl.

does when using this technique to infer the beam energy out of the rf-gun. The main error comes from possible mis-centering of the beam at the spectrometer entrance, in such a case given the initial coordinate of the beam centroid (x_0, x_0'), the horizontal beam position on the spectrometer OTR screen is:

$$x_{XS3} = R_{11}x_0 + R_{12}x_0' + R_{16}\delta_0, \tag{2}$$

wherein R_{11} and R_{12} are the transport matrix elements connecting the position to an initial position and an initial divergence, and R_{16} is the dispersion at the screen location. The quantity $\delta_0 \doteq \langle E \rangle / E_{spec} - 1$ represents the relative energy offset between the beam mean energy $\langle E \rangle$ and the energy for which the spectrometer is set E_{spec}. Then by trying to center the beam on the OTR screen an operator will make a systematic error on the relative energy offset given by:

$$\delta_0 = -\frac{1}{R_{16}}(R_{11}x_0 + R_{12}x_0'), \tag{3}$$

which translate to an energy on the estimated energy of:

$$\langle E \rangle = E_{spec}\left(1 - \frac{1}{R_{16}}(R_{11}x_0 + R_{12}x_0')\right). \tag{4}$$

For typical values ($R_{11} \simeq 0.42$, $R_{12} \simeq 0.62$ m, and $R_{16} \simeq 0.32$ m) and assuming a mis-steering in the beamline resulted in the extreme values $x_0 = 5$ mm and $x_0' = 5$ mrd, we find the systematic error to be of the order of 2% only. Hence we believe under nominal operation the method give proper values for the energy at the gun exit.

2.2 Measurements

From a series of measurements performed in autumn/winter 2003 [4, 5, 6], we constantly found, that the measured gun energy was lower that the one expected from the forward rf-power setting as already mentioned. The zero-extrapolation was performed using a linear fit of E variation versus E_{TESLA}, with a fit routine based on Reference [14]. Our measurements are gathered in Fig 3 for various setting of the rf-gun. The errorbars result from an error propagation considering a 3% systematic uncertainty on the energy measurement downstream of the TESLA-cavity.

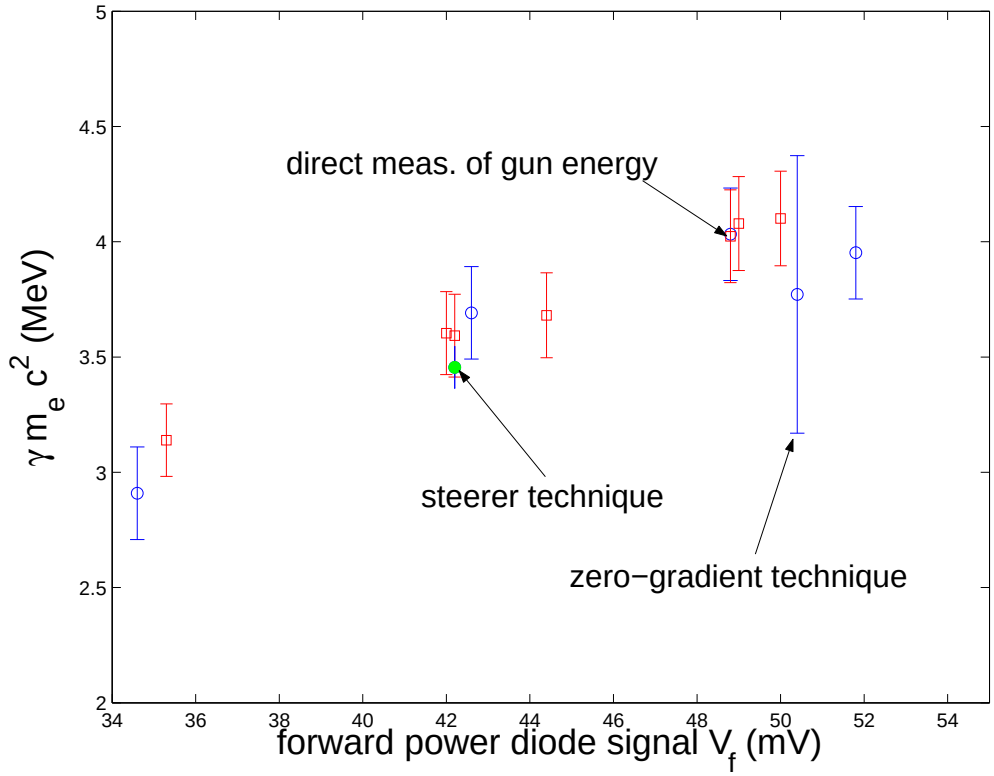

Figure 3: Beam energy at the gun exit measured for different forward rf-power (represented by the forward input power diode signal V_f). The gun energy is measured either from the TESLA cavity zero gradient interpolation method (blue circle data points) or a direct measurement after transport of the beam up to the spectrometer with the TESLA cavity turned off (red square data points). The energy measured using the magnetic properties of the steerer HTB09C is also reported for comparison (green filled circle) .

3 Measurements of gun energy with HTBC09 steerer

Instead of using the spectrometer to measure the beam energy we also attempted to use a magnetic steerer located downstream of the rf-gun. For such measurement we use the steerer HTBC09 located just upstream from the TESLA cavity. The steerer strength was varied and the so-induced position change on the screen X5 was measured. This screen is laminated with YaG:Td powder (henceforth such screens are referred to as YaG screens). For such a measurement, the steerers transverse magnetic fields (both horizontal and vertical) were measured and parametrized with the analytical approximation for the field profile resulting from coils (see more detailed discussion in [2]):

$$B(z) = B_0 + \frac{\hat{B}}{\cosh(z/a)} I, \tag{5}$$

wherein I is the excitation current and $\hat{B}$, a and B_0 are some free parameters that need to be extracted from the measurement. A fit of the measurement yielded the values $a = 4.81699$ cm and $\hat{B} = 4.2812$ G for a 1 A excitation current. The magnetic field offset is found to be

$B_0 = 0.529503$ G, a value consistent with the Earth magnetic field. The advantage of using Eq.(5) for modeling the field is that the angular kick imparted by the steerer can then be estimated analytically from:

$$\frac{dx'}{dI} = \frac{e\int_{-\infty}^{+\infty} B(z)dz}{p_{\|}} = \frac{e}{p_{\|}}\left[2a\hat{B}\arctan\left(\tanh(z/(2a))\right)\right]_{-\infty}^{+\infty} = \frac{e}{p_{\|}}\pi a\hat{B}, \tag{6}$$

that is in practical units:

$$\frac{dx'}{dI}[\mathrm{rad/A}] = \frac{1.9436\times 10^4}{p_{\|}c[\mathrm{eV}]}. \tag{7}$$

Taking into account the distance between the steerer (here we consider HTB09C) and the YaG screen X5 (L =3.729 m), one finally gets:

$$p_{\|}c[\mathrm{eV}] = \frac{7.247\times 10^4}{(dx)/(dI)}, \tag{8}$$

wherein $(dx)/(dI)$ is in units of m.A^{-1}. For a rf-gun forward power input voltage V_f=42.2 mV we measured: 3.41 and 3.50 MeV for two series of measurement reported in Fig. 4 [3]. These two measurements give results consistent with the measurement reported in the previous section (see Fig. 3).

4 Possible explanations for the low gun energy

4.1 field unbalance in the rf-gun

To study the possible implication on the field unbalance of the rf-gun, we use results from SUPERFISH calculations. For the unbalanced case we considered the unbalanced field that was simulated and found consistent with the measurements of gun 3 − obviously this represents a worst case scenario (we do not expect gun 4 to have the same deformation), but it is nevertheless instructive to consider. The field profile $E_z(r = 0, z)$ for the two considered cases are gathered in Fig 5. From these calculations, and assuming all the forward power is dissipated in the gun cavity, we can write $P_{dissip} = \kappa E_{cath}^2$, wherein E_{cath} is the amplitude of the electric field on the cathode. We get $\kappa = 1.78\times 10^{-9}$ for the balanced case and $\kappa = 3.07\times 10^{-9}$ for the unbalanced case. Using these latter values and properly scaling the peak field in the simulation we obtained (see Fig. 6) the expected total energy of the beam versus dissipated power (which should equal forward power in a perfect system).

Clearly Figure 6 demonstrates that a unbalanced field, even in the worst case scenario

	$\mathcal{E}_{stored}(mJ)$	$P_{dissip}(W)$	E_{cath} (MV/m)
balanced	5.0699	1780.5186	1.000
unbalanced	5.2522	1761.2292	0.757

Table 1: Results of SUPERFISH simulations on the balanced and unbalanced gun scenarii.

of gun 3 (where the unbalance was severe as shown by bead pull measurement [15]), does not explain the observed discrepancies between measured and expected energies from the forward rf-power.

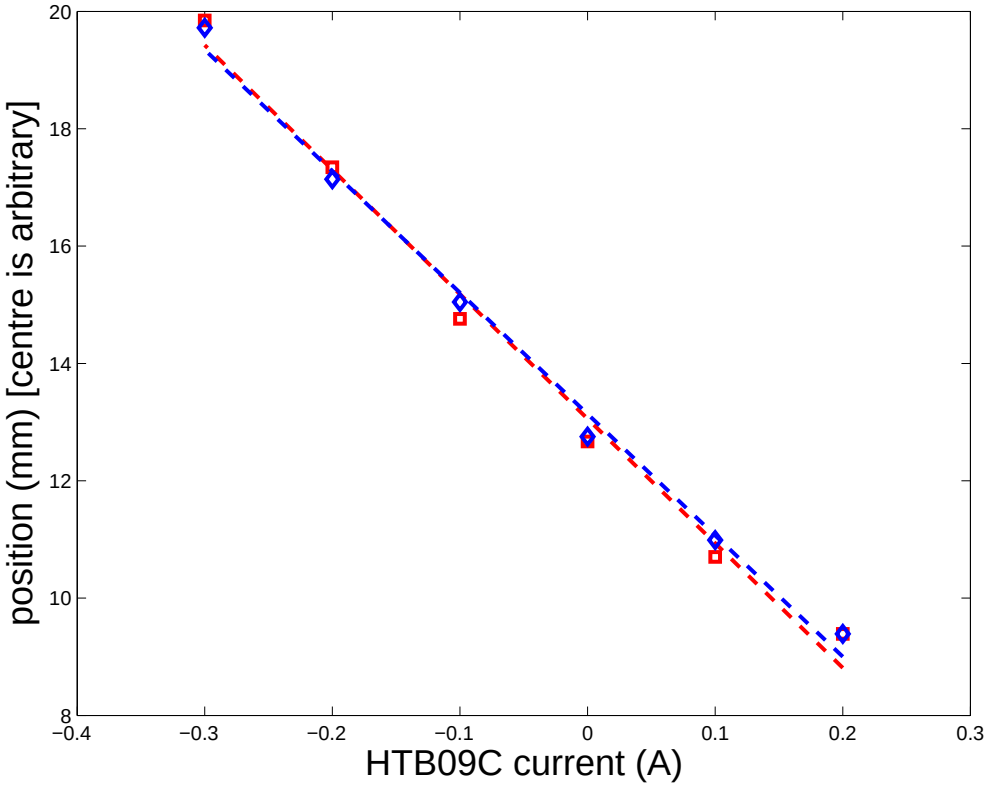

Figure 4: beam position variation on X5 YaG screen for versus excitation current in steerer HTB09C. Setting of the forward power for the rf-gun was $V_f = 42.2$ mV.

4.2 calibration of the gun rf-system

Another potential explanation for the observed discrepancies between the gun energy measured and the expected value from the forward rf-power going into the gun could be due to an erroneous calibration of forward rf-power. Some checks were done and a measurement indicated that the measured directional coupler forward coupling was 0.95 dB higher than the data posted on the directional coupler. A value of 0.95 dB implies that the actual power is $\sim$ 80% of what we thought was just due to the directional coupler. Including the waveguide loss measurement, this drops to $\sim$ 78.5%.

On another hand, the high power unloaded Q, Q_0, was measured for the cavity using a decay time measurement and assuming unity coupling (the measured reflected power was negligible). Assuming the diode detector/scope does not contribute to this measurement (previous decay measurements of the diode/scope combination with a signal generator resulted in 0.2 μs decay time), we measured a $\sim$2.6 μs decay time resulting in $Q_0 \simeq 21000$. This is 9% less than the low power Q_o measurement of 23000. This lowers the scaling factor relating the ratio between the field to the square root of the power by 4%.

Thus combining the above 3 measurements the gradient was found to be $\sim$15% lower than what was previously thought since late 90's.

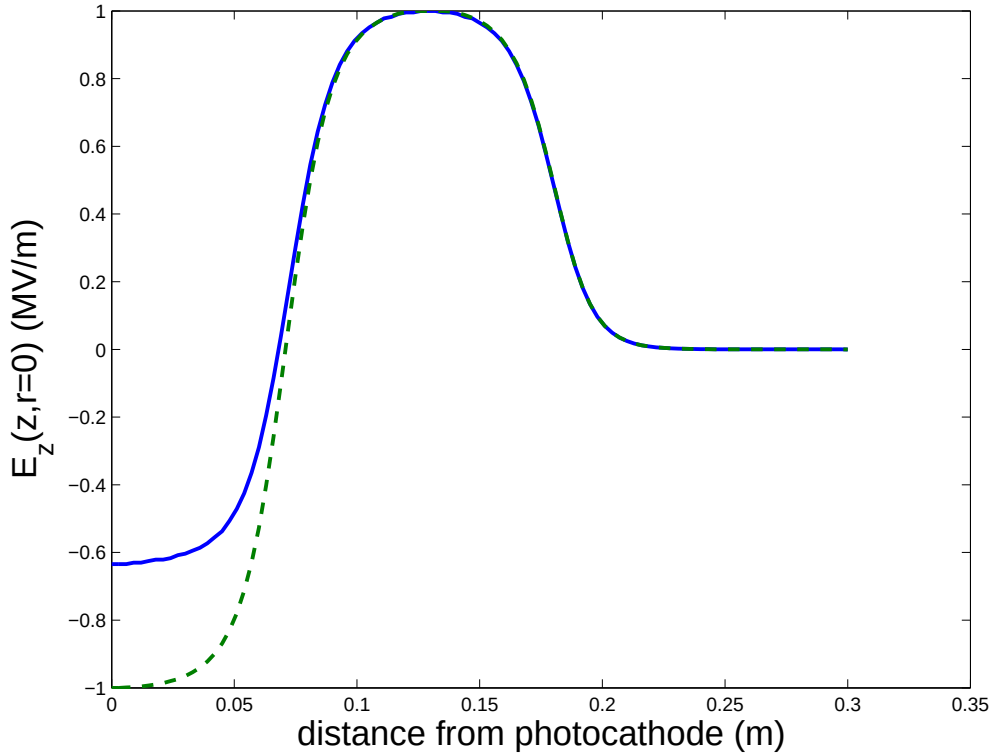

Figure 5: Comparison of the $E_z(r = 0, z)$ field profiles for the balanced (solid) and unbalanced (dashed) case considered.

4.3 spectrometer calibration

Finally the spectrometer calibration reported in Reference [7] was questioned. We thus performed a series of magnetic measurements to confirm this energy calibration of the spectrometer [12]. Different probes were used (due to availability) at various data taking time. The probes were located close to the dipole mid-plane to measure the maximum vertical component of the magnetic field and attention was paid to the probe inclination angle.

A first set of measurement [8] was performed using a uni-dimensional Hall probe [9]. The Hall probe was checked against a magnetic standard and a first measurement produced the calibration:

$$B[\mathrm{G}] = 147.58 \times I_{mac}[\mathrm{A}] - 5.49, \tag{9}$$

where I_{mac} is the set-point entered in the control system software (e.g. on the Machintosh). we also measured the current flowing in the spectrometer I_{spec} as a function of the current I_{mac} and a linear regression gave:

$$I_{mac}[\mathrm{A}] = 0.9855 \times I_{spec}[\mathrm{A}] + 0.0696. \tag{10}$$

A second series of measurement was performed using a tri-dimensional Hall probe [10] and the deduced relationship was:

$$B[\mathrm{G}] = 147.37 \times I_{spec}[\mathrm{A}] + 6.41 = 149.54 \times I_{mac}[\mathrm{A}] - 3.92. \tag{11}$$

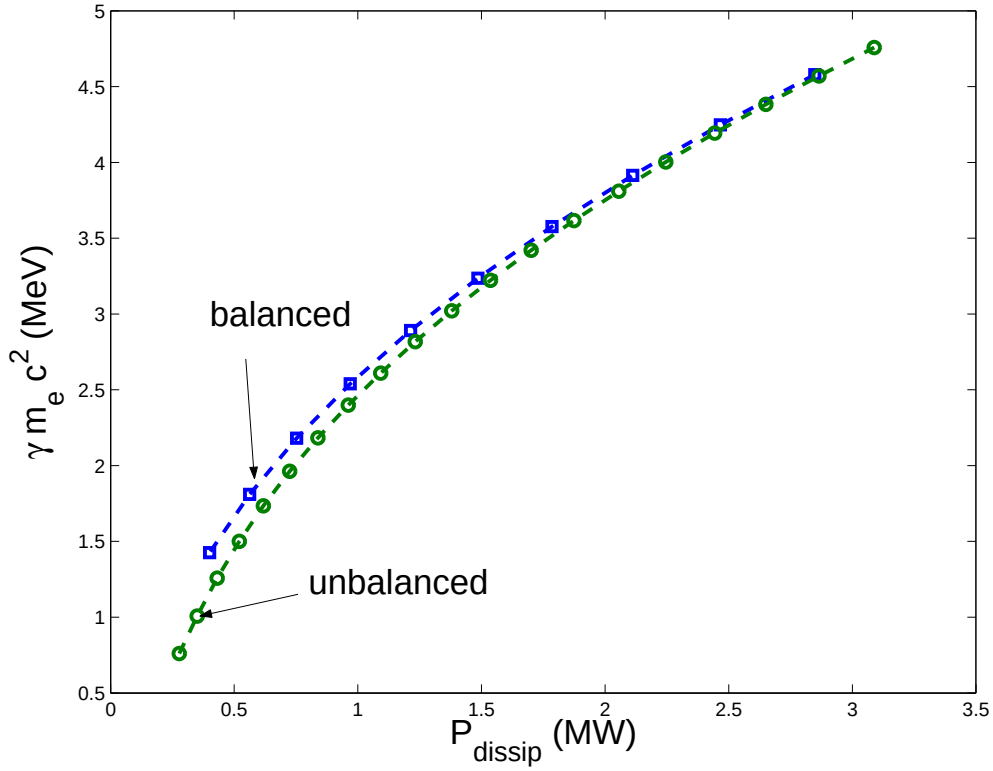

Figure 6: Expected beam energy downstream of the rf-gun versus dissipated (=forward) power for the case of balanced (blue) and unbalanced (green) field in the rf-gun.

Finally a third series of measurement was performed using a uni-dimensional Hall probe [11] that was calibrated against a nuclear magnetic resonance device. The deduced relation between the B-field and the current is:

$$B[\mathrm{G}] = 147.16 \times I_{spec}[\mathrm{A}] + 7.13 = 149.32 \times I_{mac}[\mathrm{A}] - 3.18. \tag{12}$$

All the above calibrations constant between B and I_{mac} are within 3% in agreement with the value reported in Reference [7]: $B[\mathrm{G}] = 145.6 \times I_{mac}[\mathrm{A}]$. Thus we do agree with the new spectrometer recalibration and take from Reference [7] the quoted curvature radius. However we propose to use the slightly different calibration given in Equation 12.

5 Gun energy measurement and calibration with beam of the rf-diode signal

5.1 energy measurements

In December 2003, the OTR aluminum radiator located at XS3 was replaced with a YaG screen [16]. Compared to OTR, the photon yield of such a screen is much higher thereby allowing the measurement of very low energy electron beam. The beam was transported from the gun exit up to the spectrometer with the TESLA cavity turned off. The charge per

bunch was set to $\sim$ 300 pC and transmission (measured from X1 and X8) higher than 80% could be achieved [17]. The energy of this beam was then directly measured †. Because of the low operating point of the spectrometer we are more sensitive to hysteresis of the dipole and to avoid complicating the data collection we directly installed in the spectrometer an Hall probe from which the energy was inferred using a curvature radius of 0.3697 m (see pg. 6 of Reference [7]). The resulting beam energy out of the rf-gun for different laser launch phases are reported in Figure 7.

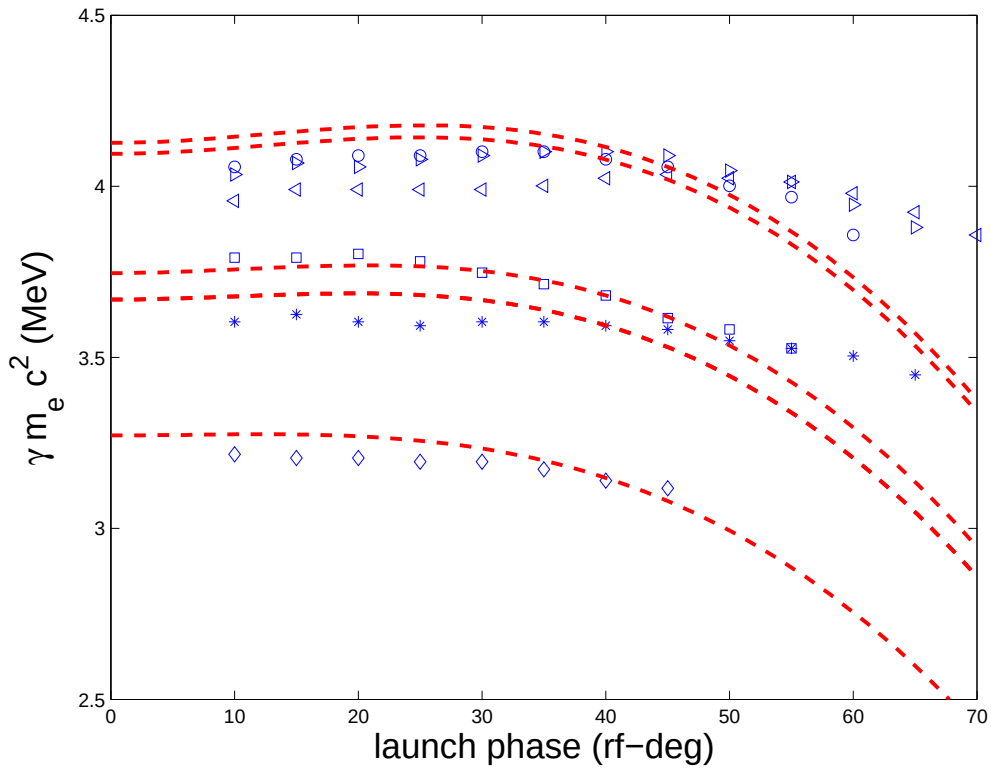

Figure 7: Beam energy out of the rf-gun versus laser launch phase. Measurements have been performed for different forward rf-power diode signal (see text).

5.2 calibration with beam of the rf-diode signal for V_f

For each of the measurement reported in the previous section, a series of simulations with different gun peak E-field were performed until the simulated energy match the experiment for $\varphi = 40°$ on all the set of measurement reported in Figure **??**. Hence we obtain a direct correspondence between forward power diode voltage and peak field on cathode for the few set-points of the gun. The question now arise on how to fit these sparse data to deduce a continuous relation between V_f and $\hat{E}_{cath}$. In Reference [13] a model of the rf-diode was introduced and the output diode voltage V_f (read on the control room oscilloscope) was

†The energy loss factor due to wakefield in the TESLA cavity is negligible − about 1 V/pC for a 1 mm (rms) long bunch.

formulated in term on input diode voltage V_{in} as follows[‡]:

$$V_{in} = \zeta_0 |V_f| + \zeta_1 \log\left(1 + \zeta_2 |V_f|\right), \tag{13}$$

where log is the Neperian logarithm (base e) and ζ_i's are constants that have been determined in Reference [13] (appendix C) directly by using a signal generator to vary $|V_{in}|$. The forward power at the gun is then given by:

$$P_f = \nu \left[\zeta_0 |V_f| + \zeta_1 \log\left(1 + \zeta_2 |V_f|\right)\right]^2, \tag{14}$$

ν is a constant that contains a numerical factor related to the conversion of voltage to power (impedance), and a numerical factor related to the fact the power computed from the voltage at the diode is attenuated. Finally, the peak field on the cathode can be written:

$$\hat{E}_{cath} = \kappa \sqrt{P_f} \doteq \tilde{\nu} \left[\zeta_0 |V_f| + \zeta_1 \log\left(1 + \zeta_2 |V_f|\right)\right], \tag{15}$$

where κ can be calculated from electromagnetic eigensolvers such as SUPERFISH. Hence we could use the ζ_i's given in Reference [13] and do a one parameter fit of V_f and $\hat{E}_{cath}$ with $\tilde{\nu}$ as a free parameter. Such a fit, presented in Fig. 8, results in a value $\tilde{\nu} = 26.6358 \pm 0.1486$. Our resulting new calibration between the output voltage of the diode (read in the control room oscilloscope) and the peak field on the cathode is:

$$\hat{E}_{cath} = 26.636 \times \left[0.0196 |V_f| + 0.0446 \log\left(1 + 3.642 |V_f|\right)\right]. \tag{16}$$

wherein E_{cath} is in MV/m and V_f in mV.

6 Energy gain in the TESLA cavity, calibration of V_t

A relation similar to Equation 13 was used for the transmitted rf-power diode signal V_t. It is interesting to calibrate with beam, the electric peak field in the TESLA cavity versus the signal V_t. We then write the energy gain in the cavity as:

$$\Delta E_{TESLA} = \tilde{\mu} \left[\xi_0 |V_t| + \xi_1 \log\left(1 + \xi_2 |V_t|\right)\right], \tag{17}$$

where the parameters ξ_i's are taken from Reference [13] (appendix C) and $\tilde{\mu}$ can be obtained from a one-variable fit of the above equation on measurement of energy dependence for different set-point of the transmitted rf-power signal diode. Such measurements are readily available (see previous sections). The result of the fit gives: $\tilde{\mu} = 5.4155 \pm 0.07124$. The corresponding calibration between the output voltage of the transmitted rf-power diode (read in the control room oscilloscope) and the energy gain provided by the cavity (assuming the beam is on-crest) is:

$$\Delta E_{TESLA} = 5.4155 \times \left[0.0366 |V_t| + 0.0675 \log\left(1 + 18.032 |V_t|\right)\right]. \tag{18}$$

wherein ΔE_{TESLA} is in MeV and V_t in mV. The corresponding peak E-field in the TESLA cavity is given by (see appendix):

$$\hat{E}_{TESLA} = 10.0904 \times \left[0.0366 |V_t| + 0.0675 \log\left(1 + 18.032 |V_t|\right)\right]. \tag{19}$$

wherein $\hat{E}_{TESLA}$ is in MV/m and V_t in mV.

[‡]This equation, developed for a simplified diode peak detector model, is different from the previous parametrization (that did not involved any physics) introduced by W. Hartung which was based on a order 8 polynomial fit of the measured diode characteristics

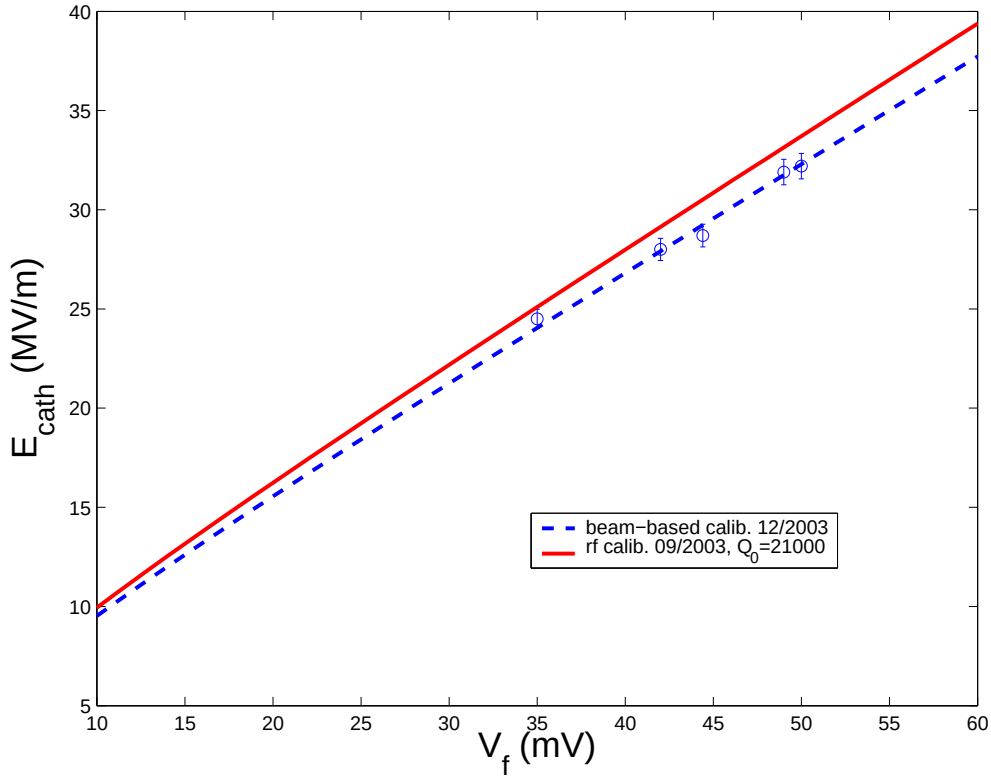

Figure 8: Accelerating peak E-field on the photo-cathode versus V_f signal. The circle results from the measurement and the dashed line is a fit of the data taking into account the peak detector diode characteristics.

7 Benchmarking of the new rf-calibrations

An experiment to measure the variation of the electron bunch time-of-flight up to the TESLA cavity was performed [18]. The launch phase was set to 25°, and for various operating field of the gun, the TESLA cavity phase is optimize to maximize the beam momentum. The observed shift of the TESLA cavity provide a measure of the variation of the time of arrival at the cavity. The results of such measurement is compared with simulation in Fig 9, the agreement between measured TESLA cavity phase shift with the one predicted using the rf and beam-based calibration are very good (note that the uncertainty on the phase is typically 1 to 5° depending on the energy spread of the beam.

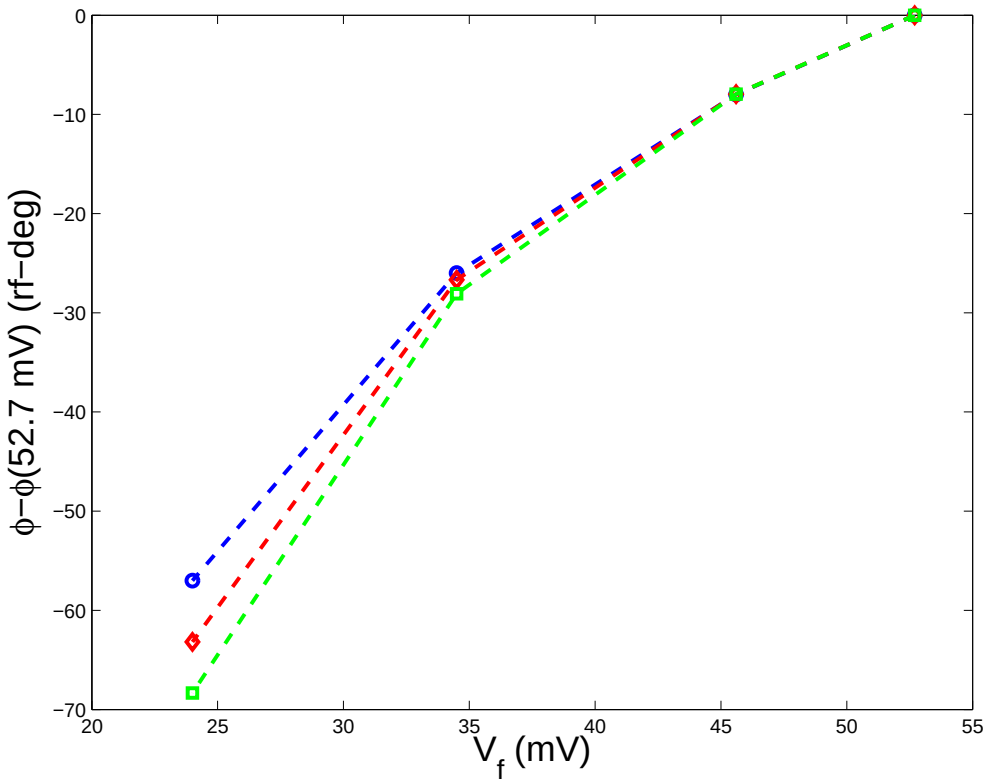

Figure 9: Relative phase shift of the TESLA cavity needed to maximize the energy versus operating V_f for the gun.

8 *In fine*

Firstly, we have measured and reproduced the magnetic field measurement performed in Reference [7] our agreement is very good and we are now convinced the previous spectrometer calibration performed in 1998 is erroneous. It should be noted that this calibration is consistent with the (independent) rf-calibration of the TESLA cavity. We propose to use the relation:

$$B[\mathrm{G}] = 149.32 \times I_{mac}[\mathrm{A}] - 3.18.$$

that is,

$$p[\mathrm{MeV/c}] = 1.619 I_{mac}[\mathrm{A}] - 0.035 \simeq 1.619 I_{mac}[\mathrm{A}].$$

We should note that we are in the process of permanently install an Hall probe in the spectrometer to constantly monitor the B-field and not have to rely on the current anymore.

Given this aforementioned spectrometer calibration, we found the beam total energy is substantially lower than the expected energy per rf-gun and TESLA cavity settings. We have found this error to be essentially due to an overestimation of the rf-gun energy. In this view we propose a new calibration of the forward power diode signal V_f using direct energy measurement of the beam:

$$\hat{E}_{cath}[\mathrm{MV/m}] = 26.636 \times [0.0196|V_f|[\mathrm{mV}] + 0.0446 \log(1 + 3.642|V_f|[\mathrm{mV}])] \,,$$

wherein $\hat{E}$ is the peak electric field on the cathode (i.e. what's is needed as an input for numerical simulation tracking programs). For completeness, we also report the latest rf calibration:

$$\hat{E}_{cath}[\mathrm{MV/m}] = 27.806 \times [0.0196|V_f|[\mathrm{mV}] + 0.0446 \log(1 + 3.642|V_f|[\mathrm{mV}])] \,.$$

Finally we noted that although the agreement is now much better, there is question regarding the accuracy of the TESLA cavity rf-calibration, for such a purpose we propose to again use direct beam energy measurement to provide a calibration of the transmitted power diode signal V_t:

$$\hat{E}[\mathrm{MV/m}] = 10.0904 \times [0.0366|V_t|[\mathrm{mV}] + 0.0675 \log(1 + 18.032|V_t|[\mathrm{mV}])].$$

wherein $\hat{E}$ is the peak electric field in the TESLA cavity (i.e. what's is needed as an input for numerical simulation tracking programs)

References

[1] e.g. see logbook #10, pg. 87, March 2002

[2] P. Piot, Y.-E. Sun, "measurement of the TESLA cavity transfer matrix" (in preparation)

[3] See logbook #13, pg. 36, August 2003 entry by P. Piot and Y.-E. Sun

[4] See logbook #13, pgs 84-86, August 2003 entry by P. Piot and Y.-E. Sun

[5] See logbook #13, pg. 133, September 2003 entry by P. Piot

[6] See logbook #13, pg. 169, October 2003 entry by N. Barov and P. Piot

[7] K. Bishofberger, "FNPL spectrometer recalibration", unpublished work available at `<http://nicadd.niu.edu/fnpl/docs/kip-spectrometer.pdf>` (August 2002)

[8] See logbook #13, pgs 116-118, October 2003 entry by N. Barov and P. Piot

[9] Hall probe borrowed from T. Johnson

[10] Hall probe lakeshore model 460, borrowed from K. Bishofberger,

[11] High Sensitivity Hall Probe DMT141 – bar code #000806, Teslameter bar – bar code #000805, borrowed from D. Orris (technical division)

[12] See logbook #13, pg. 203, November 2003 entry by N. Barov

[13] T. Berenc, "calibration of the rf power monitors for the photoinjector laboratory rf system", RF Note #044, internal FNAL RF-group technote available at `<http://www-rfi.fnal.gov/global/technotes/TN/TN044.pdf>` (August 2002)

[14] P. Bevington and D. Robinson, *Data reduction and error analysis for the physical sciences* 2nd ed., WCB/McGraw-Hill (1992)

[15] E. Thrane, "Bead pull measurement of the gun G3" unpublished work (September 2003)

[16] the YaG screen was provided by DESY-Hamburg

[17] See logbook #13, pg. 291-300, August 2003 entry by P. Piot

[18] See logbook #14, pg. 158, April 2004 entry by N. Barov

Appendix: notes on peak field and average accelerating gradient in the TESLA cavity

In this appendix, we compute the relations between energy gain, average accelerating gradient and peak accelerating field for the TESLA cavity. It is generally taken for granted that the peak field $\hat{E}$ is two times the average accelerating gradient $\bar{G}_{rf}$ for a standing wave structure accelerating an incoming relativistic beam ($\beta = 1$). Such a fact is not exactly true for a TESLA cavity as we shall see bellow.

Let $E_z(z, r = 0)$ be the on-axis longitudinal electric field in the TESLA cavity. The energy gain through the cavity, assuming a relativistic electron ($\beta = 1$) so that $t(z) = z/c$ is:

$$W = e \int_{-\infty}^{+\infty} E_z(z, r = 0) \cos(\omega t(z) + \varphi) dz \tag{20}$$

where $\omega = 2\pi f$, f being the cavity frequency. We assume from now on the electron is injected on-crest $\varphi = 0$. The above integration is numerically computed using the field profile calculated with MAFIA (see Fig. 10). The energy gain normalized to the peak field is then:

$$\frac{W}{e\max(E_z(z, r = 0))} = 0.5367 \text{ m} \tag{21}$$

The average accelerating is defined as the energy gain divided by the active length of the accelerating structure. For a 9-cells TESLA cavity the active length is:

$$l = 7 \times 115.4 + 2 \times 114.7 = 1037.2 \text{ mm}. \tag{22}$$

Hence the ratio of accelerating gradient over peak field is:

$$\frac{\bar{G}_{rf}}{e\max(E_z(z, r = 0))} = 0.5176. \tag{23}$$

Note that this number is usually taken to be 1/2.

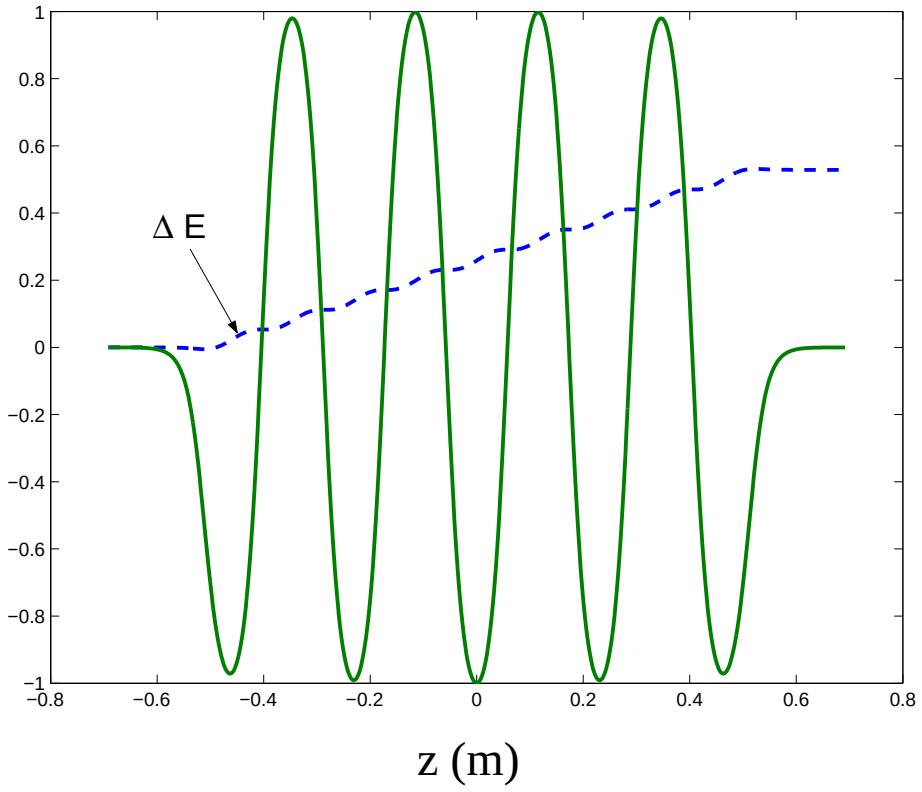

Figure 10: On-axis longitudinal electric field in the TESLA 9-cell cavity along with the corresponding energy gain for an incoming relativistic electron injected on crest.